Journal of Vacuum Science and Technology A

RESEARCH ARTICLE | AUGUST 24 2023

Vertical NiO/β-Ga_2O_3 rectifiers grown by metalorganic chemical vapor deposition

Hsiao-Hsuan Wan ; Jian-Sian Li ; Chao-Ching Chiang ; Fan Ren ; Timothy Jinsoo Yoo ; Honggyu Kim ; Andrei Osinsky ; Fikadu Alema ; Stephen J. Pearton

J. Vac. Sci. Technol. A 41, 052707 (2023)
https://doi.org/10.1116/6.0002884

JVST A
Journal of Vacuum Science & Technology A
ARTICLE
pubs.aip.org/avs/jva

Vertical NiO/β-Ga_2O_3 rectifiers grown by metalorganic chemical vapor deposition

Cite as: J. Vac. Sci. Technol. A **41**, 052707 (2023); doi: 10.1116/6.0002884
Submitted: 12 June 2023 · Accepted: 27 July 2023 ·
Published Online: 24 August 2023

View Online Export Citation CrossMark

Hsiao-Hsuan Wan,[1,a)] Jian-Sian Li,[1] Chao-Ching Chiang,[1] Fan Ren,[1] Timothy Jinsoo Yoo,[2] Honggyu Kim,[2] Andrei Osinsky,[3] Fikadu Alema,[3] and Stephen J. Pearton[2]

AFFILIATIONS

[1]Department of Chemical Engineering, University of Florida, Gainesville, Florida 32611
[2]Department of Materials Science and Engineering, University of Florida, Gainesville, Florida 32611
[3]Agnitron Technology Incorporated, Chanhassen, Minnesota 55317

[a)]**Author to whom correspondence should be addressed:** hwan@ufl.edu

ABSTRACT

The performance of vertical Schottky and NiO/β-Ga_2O_3 p-n heterojunction rectifiers in which the Ga_2O_3 was grown by metalorganic chemical vapor deposition (MOCVD) is reported. The Si-doped Ga_2O_3 drift layers employed in the study had a doping concentration of 7.6×10^{15} cm^{-3} with a thickness of approximately 6 μm. High-angle annular dark-field scanning transmission electron microscopy imaging revealed an absence of interfacial features or extended defects around the drift layer region, indicating that MOCVD provides high-quality β-Ga_2O_3 epitaxial films for fabrication of vertical rectifiers. Both Schottky and NiO/Ga_2O_3 p-n heterojunction rectifiers attained the highest reported breakdown voltage of 486 and 836 V, respectively, for this growth technique. The heterojunction rectifiers showed an on/off ratio surpassing 10^9 within the voltage range of 0 to −100 V. Additionally, the Schottky barrier diodes demonstrate an on/off ratio of up to 2.3×10^6 over the same voltage range. These findings highlight the promise of MOCVD as a growth method for the type of rectifiers needed in power converters associated with an electric vehicle charging infrastructure.

I. INTRODUCTION

β-Ga_2O_3 is a wide bandgap semiconductor (4.6–4.9 eV) with a number of attractive properties for electronic applications, including high breakdown voltage (breakdown field >8 MV/cm, leading to breakdown voltages above 8 kV),[1–3] and high radiation hardness. These properties make Ga_2O_3 a promising material for next-generation power rectifiers, which are used to convert alternating current (AC) to direct current (DC).[1]

One of the most promising methods for growing high-quality Ga_2O_3 films is metalorganic chemical vapor deposition (MOCVD).[4–17] This technique has been used to grow high-quality Ga_2O_3 films with a range of properties, including high carrier concentration, high mobility, and good crystallinity. To grow thick Ga_2O_3 films for power rectifier applications, it is important to control the growth rate and morphology of the films. The growth rate can be controlled by adjusting the deposition parameters, such as the growth temperature, pressure, and molar flow rate of the metalorganic precursors. The morphology of the films can be controlled by using a variety of techniques, such as substrate biasing, surface texturing, and postgrowth annealing. By controlling the growth rate and morphology of Ga_2O_3 films, it is possible to grow thick films with excellent properties for the type of breakdown voltages needed for power rectifier applications.[6–15] The control of morphology means that there is no need for the type of postgrowth mechanical polishing required for halide vapor phase epitaxy. Similarly, molecular beam epitaxy is generally considered to be better suited to thinner device structures, such as high electron mobility transistors because of its relatively slow growth rate.

To overcome the lack of p-type doping capability in β-Ga_2O_3, heterojunctions with p-type NiO have been demonstrated with kilovolt-class performance and a new class of bipolar operation of β-Ga_2O_3 power electronics.[4,18–25] So far, Ga_2O_3 in those structures has been grown by Halide Vapor Phase Epitaxy (HVPE), which has drawbacks in terms of rough surface morphology, requiring significant amounts of the grown layer to be planarized by chemical mechanical polishing. By contrast, MOCVD requires no such postgrowth processing.

In this paper, we present our findings on the growth and fabrication of vertical geometry NiO/Ga_2O_3 rectifiers with a high breakdown voltage (V_B) of 836 V, while Schottky rectifiers fabricated on the same drift layers exhibited a breakdown voltage of 486 V. These values represent record-breaking numbers among vertical Ga_2O_3 rectifiers grown using MOCVD technology.

II. EXPERIMENT

We fabricated both NiO/β-Ga_2O_3 heterojunction and Schottky rectifiers on the same wafer to compare their characteristics. Figure 1 shows the schematic of our vertical devices. The Si-doped β-Ga_2O_3 epitaxial layers were grown at Agnitron Technology using their Agilis 100 MOCVD reactor on Sn doped (010) β-Ga_2O_3 substrates (Novel Crystal Technology) of size $15 \times 10\,mm^2$. The substrate was etched in an HF for 30 min before loading into the reactor for the epilayer growth to remove native oxide and any other surface contamination. The etch rate of the substrate is negligible for this step. Triethylgallium (TEGa), pure oxygen (O_2), and silane balanced in N_2 (SiH_4/N_2) were used as precursors, and argon (6 N) was used as a carrier gas. The growth pressure, substrate temperature, and O_2/TEGa ratio used to grow the layers were 15 Torr, 810 °C, and ∼400. The entire structure consisted of a 0.1 μm-thick n + β-Ga_2O_3 current spreading layer ($N_D = 5 \times 10^{18}\,cm^{-3}$), followed by ∼6 μm thick lightly doped β-Ga_2O_3 drift layers ($N_D = 7.6 \times 10^{15}\,cm^{-3}$), measured by capacitance-voltage (C-V) data. This was consistent with the Hall effect data, showing a similar electron density to the donor density and a mobility of ∼150 cm^2/V s, as described in detail previously.[26] This indicates that there is little compensation by acceptors. The drift layer was grown at a ∼1 μm/h growth rate, and the doping concentration in the layer was achieved by introducing silane with a molar flow rate of $4 \times 10^{-12}\,mol\,min^{-1}$ into the reactor. The growth rates were obtained from the film thicknesses measured on β-Ga_2O_3 films grown on coloaded sapphire substrates by cross-sectional field emission scanning electron microscopy imaging. No N_2 was incorporated into the films to the sensitivity of secondary ion mass spectrometry ($10^{17}\,cm^{-3}$).

Figure 2 shows the surface morphology of the film as measured by atomic force microscopy (AFM). The AFM image was taken from a $5 \times 5\,\mu m^2$ scan area and showed typical surface morphology obtained from MOCVD-grown β-Ga_2O_3 epitaxial films.[4,5,7] The film is smooth with an RMS roughness of 0.6 nm. The obtained smoothness of the film for such a thick layer is attributed to the low growth pressure used in this work that likely minimized gas phase reaction in the reactor and reduced the formation of particles that can cause the nucleation of defects.[26]

Ti/Au (=20 nm/80 nm) was deposited for Ohmic contact on the whole rear side of the Ga_2O_3 substrate by an e-beam evaporator, followed by annealing at 550 °C for 3 min under N_2. The front side of the sample was cleaned by UV/ozone exposure for 15 min before NiO deposition. The NiO bilayer was fabricated on the epi layer utilizing RF magnetron sputtering employing NiO targets at a pressure of 3 mTorr and a frequency of 13.56 MHz. The doping level in the NiO was controlled within the range of 1.0×10^{18} to $2.6 \times 10^{19}\,cm^{-3}$ (Hall measurement) by adjusting the Ar/O_2 gas ratio during sputtering. The mobility, as also determined by Hall measurements, was found to be less than $1\,cm^2\,V^{-1}\,s^{-1}$. After NiO deposition, we annealed the sample at 300 °C for 1 min under O_2. The gas flow rate governs the stoichiometry of the film and the abundance of point defects that determine the effective carrier concentration. An extensively comprehensive analysis of the characteristics of NiO deposited on Ga_2O_3 has been previously provided.[27] Last, we deposited Ni/Au (20 nm/80 nm) as the contact metal on the top of the NiO layer. The details on the fabrication of the Schottky and heterojunction rectifiers have been given previously.[3,24,25]

A cross-sectional microscopy sample of the β-Ga_2O_3 sample was prepared along the [001] zone axis using a FEI Helios Nanolab 600i Dual Beam focused ion beam (FIB) system for scanning transmission electron microscopy (STEM). High-angle annular dark-field imaging in STEM (HAADF-STEM) was performed using a 200 kV Themis Z (Thermo Scientific) at 25 pA with a semiconvergence angle of 22 mrad.

The current density–voltage (J–V) characteristics were measured on a Tektronix 370A curve tracer and Agilent 4156C. The Glassman high voltage power supply was used for breakdown voltage measurement. The high bias measurements were performed in Fluorinert. The on-resistance values were calculated as the slope of forward current density. We also subtracted the resistance of the cable, probe and chuck, which was around 10 Ω. In addition, the

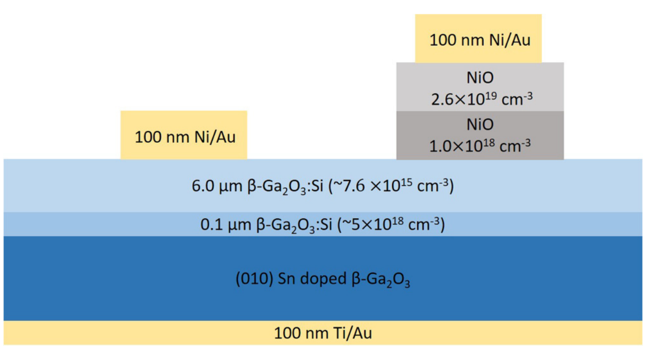

FIG. 1. Schematic of Ga_2O_3 SBD and HJD.

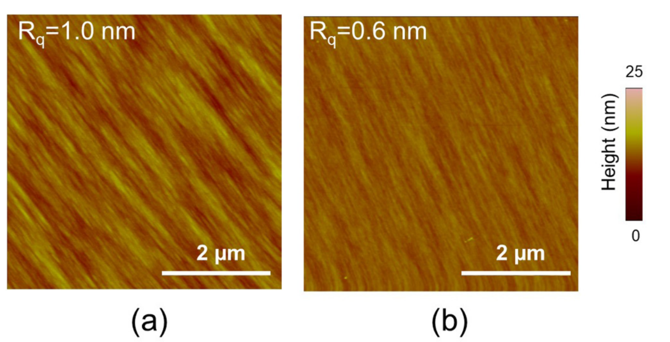

FIG. 2. 2D AFM image of the MOCVD-grown (010) β-Ga_2O_3 epitaxial film taken from a scan area of $5 \times 5\,\mu m^2$ with an RMS surface roughness of 0.6 nm.

capacitance-voltage (C-V) measurement of the β-Ga_2O_3 HJD was performed to get the carrier concentration of the buffer layer by Agilent 4284A. We set the capacitor and resistor as parallel for the measurement. The oscillator frequency is 1.00×10^6 Hz, and the voltage level is 1 V. The setup has been described in detail previously.[28,29]

III. RESULTS AND DISCUSSION

According to the known stack structure of the device, HAADF-STEM imaging was focused on the drift layer region around 6 μm below the surface of the device. An appropriately sized microscopy sample along the [001] zone axis was prepared to allow for ample room around the drift layer for thorough imaging. A low-magnification HAADF-STEM image in Fig. 3(a) reveals no indication of the drift layer 6 μm below the surface. The contrast around that section of the lamella, marked by the orange arrow, is relatively uniform. Figures 3(b) and 3(c) progressively portray higher-magnification HAADF-STEM images revealing the pristine atomic structure of the drift layer. Figure 3(d) shows the atomic model of the [001] zone axis of β-Ga_2O_3 for comparison. Overall, no interfacial features or extended defects were observed around the drift layer region, thus indicative of a high-quality β-Ga_2O_3 epitaxial film grown by the MOCVD growth technique. We have previously published detailed images of the NiO/Ga_2O_3 region.[24]

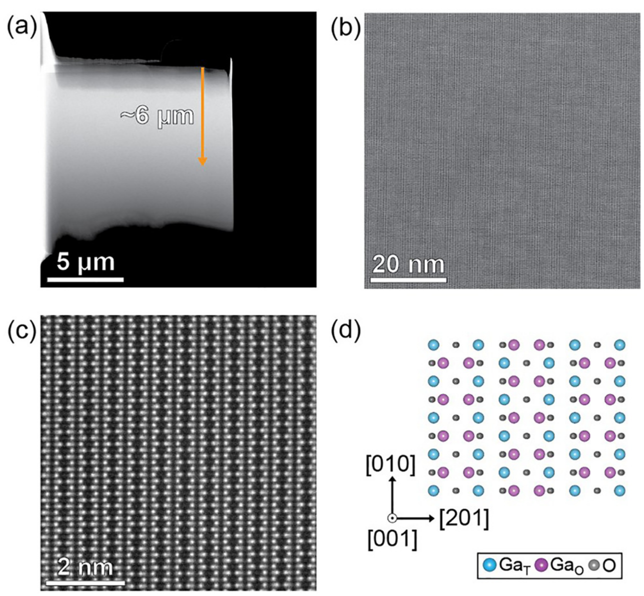

FIG. 3. (a) Low-magnification HAADF-STEM image showing an entire TEM lamella with an orange arrow marking the region 6 μm below the surface where the drift layer is expected. Note that the intensity variation near the top of the TEM lamella arises from the thickness variation during the ion milling process. (b) Medium-magnification HAADF-STEM image about the top of the drift layer. (c) High-magnification HAADF-STEM image of the β-Ga_2O_3 atomic structure projected along [001]. (d) Atomic model of the β-Ga_2O_3 structure for comparison. Note that no interfacial features or extended defects were observed in (a)–(c), thus indicating pristine growth quality.

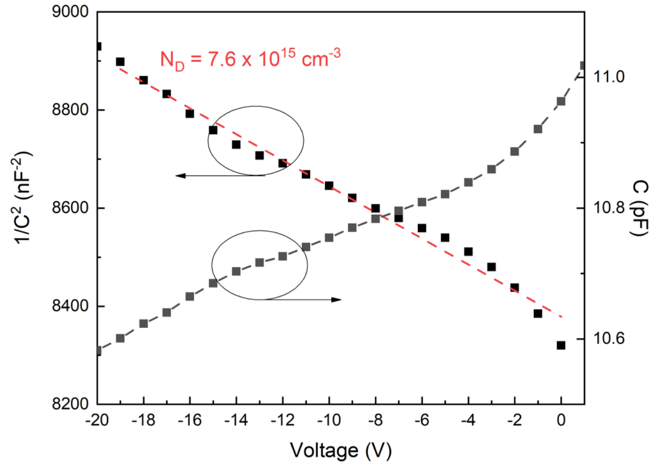

FIG. 4. C-V characteristics for determining carrier concentration of the drift layer.

Figure 4 shows the $1/C^2$-V and C-V plots. The carrier concentration of the buffer layer is 7.6×10^{15} cm^{-3}. Figure 5 illustrates the forward current densities and on-state resistances (R_{on}) for both the Schottky barrier diode (SBD) and the heterojunction diode (HJD). The forward current density is 25 and 2 A/cm^2, respectively. The R_{on} value for the Schottky barrier diode is measured at 259 mΩ cm^2, whereas the heterojunction diode exhibits a R_{on} of 2130 mΩ cm^2. While the on-resistances are higher than for state-of-the-art HVPE devices, they show an advance over previous MOCVD results.

In Fig. 6, we present the diode on/off ratio for both SBD and HJD. The on/off ratio is another figure of merit in that having high on-current and low leakage current in a reverse bias is desirable

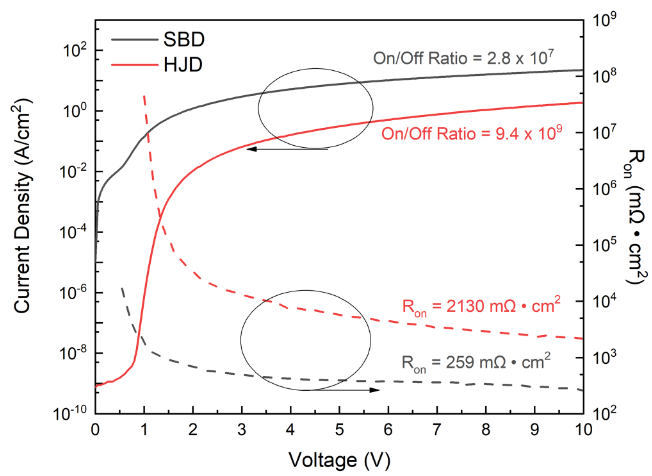

FIG. 5. Forward current density and on-state resistance for both Ga_2O_3 SBD and HJDs.

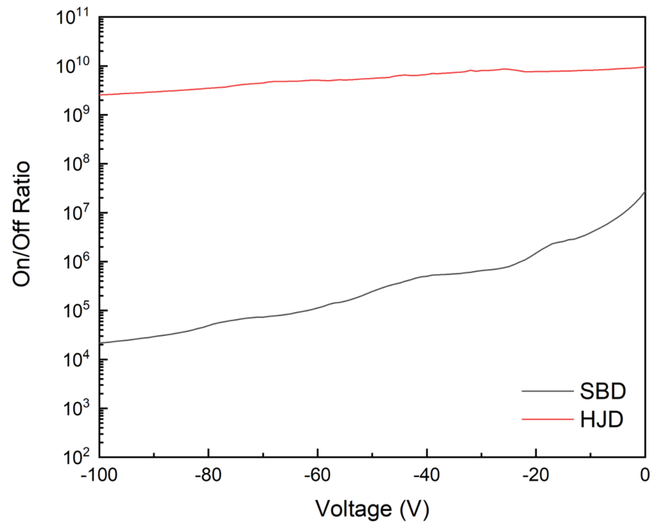

FIG. 6. On/off ratio when switching from +10 V to the voltage shown on the *x* axis.

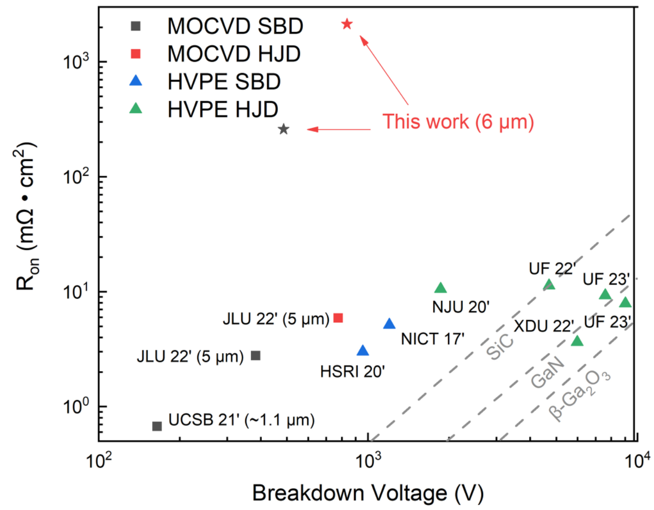

FIG. 8. Compilation of reported R_{on}-V_B values for recent Ga_2O_3-based vertical rectifiers. The MOCVD growth Ga_2O_3 devices are labeled as squares, while the HVPE devices were triangles. The SBD and HJD were also labeled with different colors. This work shows the highest reported breakdown voltages for both MOCVD growth Ga_2O_3 SBD and HJD devices.

and is defined as the ratio observed when transitioning from a forward voltage of +10 V to reverse voltages ranging from 0 to −100 V, as indicated on the *x* axis. The heterojunction diode demonstrates an impressive on/off ratio of over 10^9 within the voltage range of 0 to −100 V. Similarly, the Schottky barrier diode exhibits a substantial on/off ratio of up to 2.3×10^6.

The breakdown voltages can be derived from the reverse I-V plots, as shown in Fig 7. The breakdown voltages were also measured by Glassman, which is different from the one we measured

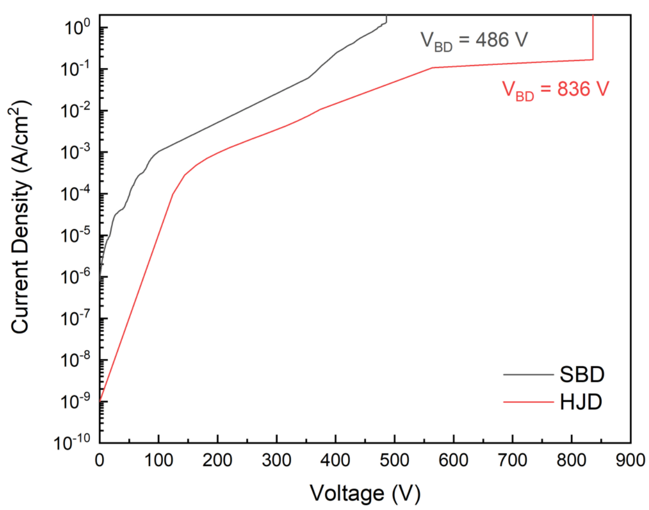

FIG. 7. Reverse I-V characteristics of rectifiers, showing the associated breakdown voltages.

from the reverse I-V. Due to the limitation of the instrument, we combined the result from a Tektronix 370A curve tracer and Glassman to perform the whole figure. These values are higher than previous reports for MOCVD devices, signifying improvement in achieving thick layers with low carrier density and smooth morphology. However, they still lag behind the HVPE results.

The maximum breakdown voltage we obtained for SBD is 486 V and for HJD is 836 V. The breakdown voltages of both SBD and HJD are the highest compared to the best reported value of MOCVD-grown β-Ga_2O_3 rectifiers. Jiao *et al.*[30] reported the breakdown voltage as 380 and 740 V for SBD and HJD, respectively. Figure 8 is the compilation of reported R_{on}-V_B values from different institutions for Ga_2O_3-based devices.[4,12,24,25,30–37] In this figure, the MOCVD-grown Ga_2O_3 devices were classified as squares, while the HVPE devices were represented by triangles. Different colors were assigned to the Schottky barrier diodes (SBDs) and heterojunction diodes (HJDs) for easy differentiation. Notably, the research findings revealed the highest reported breakdown voltages for both MOCVD-grown Ga_2O_3 SBD and HJD devices. Note that the results for currently available MOCVD devices are significantly lagging the HVPE devices, but the interest in the development of the former stems from the much better morphology; removing the need for postgrowth chemical mechanical polishing that is a requirement to planarize HVPE films would have significant advantages. This polishing leaves cracks and defects on the surface, which limit device yield, as recently reported by Sdoeung *et al.*[38]

IV. SUMMARY AND CONCLUSIONS

Our results show that Ga_2O_3 epitaxial films grown by MOCVD are promising for next-generation power rectifiers.

HAADF-STEM images showed that no interfacial features or extended defects were observed around the drift layer region, indicating the exceptional film. We performed both Schottky and NiO/Ga_2O_3 p-n heterojunction rectifiers to show outstanding characteristics of MOCVD-grown Ga_2O_3 devices. The forward current densities of our devices are 25 and 2 A/cm^2 for SBD and HJD, respectively. The heterojunction diode showcases a remarkable on/off ratio exceeding 10^9 across the voltage spectrum of 0 to −100 V. Likewise, the Schottky barrier diode displays a significant on/off ratio of up to 2.3×10^6. Significantly, we have successfully attained impressive breakdown voltages of 486 V in SBD and 836 V in HJD. These achievements represent the highest reported breakdown voltages observed to date among Schottky and NiO/Ga_2O_3 heterojunction rectifiers, where the Ga_2O_3 drift layers were grown using MOCVD. Moreover, among all MOCVD-grown Ga_2O_3-based p-n diodes, our study introduces a highly desirable design strategy for NiO/Ga_2O_3 structures, resulting in the attainment of the highest achievable breakdown voltage.

ACKNOWLEDGMENTS

General MOCVD process development at Agnitron has been partially supported by the Office of Naval Research (ONR, Program Manager: Mr. Lynn Petersen) and AFWERX through Contract Nos. N6833518C0192 and FA864921P0304, respectively.

AUTHOR DECLARATIONS

Conflict of Interest

The authors have no conflicts to disclose.

Author Contributions

Hsiao-Hsuan Wan: Conceptualization (equal); Data curation (equal); Formal analysis (equal); Funding acquisition (equal); Investigation (equal); Methodology (equal); Project administration (equal); Resources (equal); Software (equal); Supervision (equal); Validation (equal); Visualization (equal); Writing – original draft (equal); Writing – review & editing (equal). **Jian-Sian Li:** Conceptualization (equal); Data curation (equal); Formal analysis (equal); Funding acquisition (equal); Investigation (equal); Methodology (equal); Project administration (equal); Resources (equal); Software (equal); Supervision (equal); Validation (equal); Visualization (equal); Writing – original draft (equal); Writing – review & editing (equal). **Chao-Ching Chiang:** Conceptualization (equal); Data curation (equal); Formal analysis (equal); Funding acquisition (equal); Investigation (equal); Methodology (equal); Project administration (equal); Resources (equal); Software (equal); Supervision (equal); Validation (equal); Visualization (equal); Writing – original draft (equal); Writing – review & editing (equal). **Fan Ren:** Conceptualization (equal); Data curation (equal); Formal analysis (equal); Funding acquisition (equal); Investigation (equal); Methodology (equal); Project administration (equal); Resources (equal); Software (equal); Supervision (equal); Validation (equal); Visualization (equal); Writing – original draft (equal); Writing – review & editing (equal). **Timothy Jinsoo Yoo:** Conceptualization (equal); Data curation (equal); Formal analysis (equal); Funding acquisition (equal); Investigation (equal); Methodology (equal); Project administration (equal); Resources (equal); Software (equal); Supervision (equal); Validation (equal); Visualization (equal); Writing – original draft (equal); Writing – review & editing (equal). **Honggyu Kim:** Conceptualization (equal); Data curation (equal); Formal analysis (equal); Funding acquisition (equal); Investigation (equal); Methodology (equal); Project administration (equal); Resources (equal); Software (equal); Supervision (equal); Validation (equal); Visualization (equal); Writing – original draft (equal); Writing – review & editing (equal). **Andrei Osinsky:** Conceptualization (equal); Data curation (equal); Formal analysis (equal); Funding acquisition (equal); Investigation (equal); Methodology (equal); Project administration (equal); Resources (equal); Software (equal); Supervision (equal); Validation (equal); Visualization (equal); Writing – original draft (equal); Writing – review & editing (equal). **Fikadu Alema:** Conceptualization (equal); Data curation (equal); Formal analysis (equal); Funding acquisition (equal); Investigation (equal); Methodology (equal); Project administration (equal); Resources (equal); Software (equal); Supervision (equal); Validation (equal); Visualization (equal); Writing – original draft (equal); Writing – review & editing (equal). **Stephen J. Pearton:** Conceptualization (equal); Data curation (equal); Formal analysis (equal); Funding acquisition (equal); Investigation (equal); Methodology (equal); Project administration (equal); Resources (equal); Software (equal); Supervision (equal); Validation (equal); Visualization (equal); Writing – original draft (equal); Writing – review & editing (equal).

DATA AVAILABILITY

The data that support the findings of this study are available within the article.

REFERENCES

[1]J. Zhang *et al.*, Nat. Commun. **13**, 3900 (2022).
[2]C. Wang *et al.*, J. Phys. D: Appl. Phys. **54**, 243001 (2021).
[3]J.-S. Li, C.-C. Chiang, X. Xia, H.-H. Wan, F. Ren, and S. J. Pearton, J. Vac. Sci. Technol. A **41**, 030401 (2023).
[4]Y. Zhang, F. Alema, A. Mauze, O. S. Koksaldi, R. Miller, A. Osinsky, and J. S. Speck, APL Mater. **7**, 022506 (2019).
[5]F. Alema, Y. Zhang, A. Osinsky, N. Valente, A. Mauze, T. Itoh, and J. S. Speck, APL Mater. **7**, 121110 (2019).
[6]F. Alema, Y. Zhang, A. Osinsky, N. Orishchin, N. Valente, A. Mauze, and J. S. Speck, APL Mater. **8**, 021110 (2020).
[7]F. Alema, Y. Zhang, A. Mauze, T. Itoh, J. S. Speck, B. Hertog, and A. Osinsky, AIP Adv. **10**, 085002 (2020).
[8]F. Alema, T. Itoh, S. Vogt, J. S. Speck, and A. Osinsky, Jpn. J. Appl. Phys. **61**, 100903 (2022).
[9]X. Du, W. Mi, C. Luan, Z. Li, C. Xia, and J. Ma, J. Cryst. Growth **404**, 75 (2014).
[10]Y. Yao, S. Okur, L. A. M. Lyle, G. S. Tompa, T. Salagaj, N. Sbrockey, R. F. Davis, and L. M. Porter, Mater. Res. Lett. **6**, 268 (2018).
[11]G. Wagner, M. Baldini, D. Gogova, M. Schmidbauer, R. Schewski, M. Albrecht, Z. Galazka, D. Klimm, and R. Fornari, Phys. Status Solidi A **211**, 27 (2014).
[12]G. Seryogin, F. Alema, N. Valente, H. Fu, E. Steinbrunner, A. T. Neal, S. Mou, A. Fine, and A. Osinsky, Appl. Phys. Lett. **117**, 262101 (2020).
[13]P. P. Sundaram, F. Alema, A. Osinsky, and S. J. Koester, J. Vac. Sci. Technol. A **40**, 043211 (2022).

[14]E. Farzana, F. Alema, W. Y. Ho, A. Mauze, T. Itoh, A. Osinsky, and J. S. Speck, Appl. Phys. Lett. **118**, 162109 (2021).
[15]L. Meng, Z. Feng, A. F. M A. U. Bhuiyan, and H. Zhao, Cryst. Growth Des. **22**, 3896 (2022).
[16]S. T. Ngo, C.-H. Lu, F.-G. Tarntair, S.-T. Chung, T.-L. Wu, and R.-H. Horng, Discov. Nano **18**, 79 (2023).
[17]A. F. M, Anhar Uddin Bhuiyan, Z. Feng, L. Meng, and H. Zhao, J. Appl. Phys. **133**, 211103 (2023).
[18]F. Zhou *et al.*, Appl. Phys. Lett. **119**, 262103 (2021).
[19]C. Wang *et al.*, IEEE Electron Device Lett. **42**, 485 (2021).
[20]*Ultrawide Bandgap* β*-*Ga_2O_3 *Semiconductor: Theory and Applications*, edited by J. S. Speck and E. Farzana (AIP Publishing, Melville, NY, 2023).
[21]Y. Lv *et al.*, IEEE Trans. Power Electron. **36**, 6179 (2021).
[22]X. Lu, X. Zhou, H. Jiang, K. W. Ng, Z. Chen, Y. Pei, K. M. Lau, and G. Wang, IEEE Electron Device Lett. **41**, 449 (2020).
[23]C. Liao *et al.*, IEEE Trans. Electron Devices **69**, 5722 (2022).
[24]J.-S. Li, H.-H. Wan, C.-C. Chiang, X. Xia, T. J. Yoo, H. Kim, F. Ren, and S. J. Pearton, Crystals **13**, 886 (2023).
[25]J.-S. Li, C.-C. Chiang, X. Xia, T. J. Yoo, F. Ren, H. Kim, and S. J. Pearton, Appl. Phys. Lett. **121**, 042105 (2022).
[26]F. Alema, G. Seryogin, and A. Osinsky, "MOCVD growth of β-Ga_2O_3 epitaxy," in *Ultrawide Bandgap* β*-*Ga_2O_3 *Semiconductor: Theory and Applications*, edited by J. S. Speck and E. Farzana (AIP Publishing, Melville, NY, 2023), pp. 3-1–3-34.
[27]S. Nakagomi, T. Yasuda, and Y. Kokubun, Phys. Status Solidi B **257**, 1900669 (2020).
[28]J. Yang *et al.*, Proc. SPIE **10919**, 1091916 (2019).
[29]R. Sharma, M. Xian, C. Fares, M. E. Law, M. Tadjer, K. D. Hobart, F. Ren, and S. J. Pearton, J. Vac. Sci. Technol. A **39**, 013406 (2021).
[30]T. Jiao, W. Chen, Z. Li, Z. Diao, X. Dang, P. Chen, X. Dong, Y. Zhang, and B. Zhang, Materials **15**, 8280 (2022).
[31]Q. Yan *et al.*, Appl. Phys. Lett. **118**, 122102 (2021).
[32]Y. Wang *et al.*, IEEE Electron Device Lett. **41**, 131 (2020).
[33]Y. Wang *et al.*, IEEE Trans. Power Electron. **37**, 3743 (2022).
[34]K. Konishi, K. Goto, H. Murakami, Y. Kumagai, A. Kuramata, S. Yamakoshi, and M. Higashiwaki, Appl. Phys. Lett. **110**, 103506 (2017).
[35]Q. He *et al.*, IEEE Electron Device Lett. **43**, 264 (2022).
[36]H. H. Gong *et al.*, Appl. Phys. Lett. **118**, 202102 (2021).
[37]H. H. Gong, X. H. Chen, Y. Xu, F.-F. Ren, S. L. Gu, and J. D. Ye, Appl. Phys. Lett. **117**, 022104 (2020).
[38]S. Sdoeung, K. Sasaki, K. Kawasaki, J. Hirabayashi, A. Kuramata, and M. Kasu, Jpn. J. Appl. Phys. **62**, 071001 (2023).